RESEARCH ARTICLE | NOVEMBER 15 2023

Quantitative magnetization measurements of magnetic particles with FePt standard samples ⊕ ⊘

Rui Luo ⓘ ; Qian Wang ⓘ ; Yu Lu; Feng Xu ⓘ ; Zhe Guo; Fei Xue ⓘ ; Long You ⓘ ; Jinquan Liu ⓘ ;
Pengshun Luo ✉ ⓘ

Check for updates

View Online   Export Citation   CrossMark

Quantitative magnetization measurements of magnetic particles with FePt standard samples Ⓕ

View Online   Export Citation   CrossMark

Rui Luo,[1] Ⓘ Qian Wang,[1] Ⓘ Yu Lu,[1] Feng Xu,[2] Ⓘ Zhe Guo,[3,4] Fei Xue,[2] Ⓘ Long You,[3] Ⓘ Jinquan Liu,[1] Ⓘ
and Pengshun Luo[1,a) Ⓘ

AFFILIATIONS

[1]MOE Key Laboratory of Fundamental Physical Quantities Measurement, Hubei Key Laboratory of Gravitation and Quantum
Physics, PGMF and School of Physics, Huazhong University of Science and Technology, Wuhan 430074, China
[2]School of Physics, Hefei University of Technology, Hefei, Anhui 230601, China
[3]School of Integrated Circuits, Huazhong University of Science and Technology, Wuhan 430074, China
[4]School of Microelectronics, Hubei University, Wuhan 430062, China

a)Author to whom correspondence should be addressed: pluo2009@hust.edu.cn

ABSTRACT

Micrometer-sized magnetic particles have been widely used in magnetic force microscopy, magnetic resonance force microscopy, and bio-
sensing. To quantitatively interpret the data obtained with magnetic particles, it is important to know the magnetic properties of the parti-
cles. However, the magnetic moment of individual particle is usually too small to be measured by common instruments for samples with
large volume. Here, we present a method to characterize magnetic microspheres using patterned FePt thin films as standard samples. The
FePt thin film in the $L1_0$ phase has perpendicular magnetic anisotropy, and the patterned features can be magnetized to near single-domain
magnets, which make them suitable standards for magnetic sphere calibration with magnetic force microscopy. Multiple linear regression is
used to analyze the frequency shift images and obtain the effective dipole moment of the spheres. The position of the dipole moment is
obtained by minimizing the residuals in multiple linear regression with a gradient descent algorithm. Three NdFeB spheres of different
diameters were measured. It was found that the magnetization increases with the increase in the diameter of the sphere, possibly due to the
weakening of ferromagnetism on the surface.

Published under an exclusive license by AIP Publishing. https://doi.org/10.1063/5.0173461

I. INTRODUCTION

Magnetic particles have been used as magnetic tweezers[1] as
well as probes in magnetic force microscopy (MFM)[2] and magnetic
resonance force microscopy.[3–6] They have also been widely used in
biomedical applications, such as biological sensing,[7,8] drug deliv-
ery,[9] and agents for magnetic imaging.[10] Among those applications,
it is critical to know the magnetic properties of the particles, espe-
cially in the application of quantitative measurements. However,
the magnetic moment of individual particle is very tiny; for
example, the magnetic moment of a ferromagnetic particle with a
diameter of $1\,\mu m$ is on the order of $10^{-13}\,A\,m^2$. This is far below
the sensitivity of commonly used magnetic measuring instruments,
such as superconducting quantum interference device (SQUID)
magnetometry and vibrating sample magnetometry.

Many methods have been developed for magnetic measure-
ment of small samples.[11] The magnetic moment of small samples
can be measured with cantilever magnetometry,[12–18] where the
torque exerting on the sample in a uniform magnetic field is mea-
sured with a sensitive cantilever. A sensitivity better than $10^4\,\mu_B$
was achieved with a field of $60\,kOe$.[15] Instead of applying a
uniform magnetic field, the alternating-gradient magnetometer
measures the dynamic force on a vibrating magnetic sample in an
alternating gradient field, and a sensitivity of $10^{-15}\,A\,m^2/\sqrt{Hz}$ is
achievable.[19,20] A novel magnetometer using a current flowing
force sensor was also developed to measure the z-component of the
micro-particles' magnetic moment.[21]

The calibration of MFM probes has been conducted using well-
defined current carrying wire loops, which were fabricated with
lithography.[22–29] The current-driven wires create inhomogeneous

stray fields, which can be calculated precisely based on the geometry and the applied current. The force on the probes is proportional to the magnetic field gradient; thus, the magnetic field can be imaged by MFM. With this method, the magnetic properties of the probe can be characterized as a function of an external magnetic field.[23] The MFM probes can also be calibrated with standard samples with well-known magnetization, such as dispersed magnetic nanoparticles on silicon substrate,[30] patterned exchanged biased magnetic layer stripes,[31] array of rectangular ferromagnetic thin film elements,[32] and single-domain uniformly magnetized CoPt dots.[33] Among them, CoPt dots have 100% remnant magnetization and large coercivity so that their magnetization is robust and can be well characterized using SQUID magnetometry.

In this paper, we present a method to characterize the effective magnetic moment of ferromagnetic microspheres using specially designed calibration samples. We intend to develop a method that can be used in an atomic force microscope (AFM) without the need for additional modules. In our application, the magnetic microsphere is attached on the end of a cantilever and used as a probe to search for new interactions beyond the standard model of particle physics.[34] The calibration sample is made of an array of micrometer-sized FePt squares, which is fabricated with photolithography. The FePt thin film is in its $L1_0$ phase and exhibits perpendicular magnetic anisotropy so that it can be magnetized in a direction normal to the sample surface. We analyze the MFM image by multiple linear regression to obtain the magnetic moment of the sphere and obtain the position of the effective magnetic dipole by the gradient descent algorithm.

II. EXPERIMENTAL DETAILS

A. Principle and methods

Here, we measure the magnetic interaction through the frequency shift (Δf) of the cantilever's resonance in the frequency modulation AFM mode (see Fig. 1). The frequency shift Δf is related to the force gradient $\partial F/\partial z$ by

$$\Delta f = -\frac{f_0}{2k}\frac{\partial F}{\partial z},\tag{1}$$

where k is the cantilever's spring constant and f_0 is its resonant frequency. Assuming that the magnetic sphere is represented effectively by a magnetic dipole moment $\vec{m}$ at position $\vec{r}_m = (x_m, y_m, z_m)$, the magnetic potential energy between the probe and the sample can be written as $U = -\vec{m}\cdot\vec{B}$, where $\vec{B}$ is given by the integral

$$\vec{B}(\vec{r}_m) = -\frac{\mu_0}{4\pi}\int\frac{3\hat{r}(\hat{r}\cdot\vec{M}) - \vec{M}}{r^3}\,dV,\tag{2}$$

where μ_0 is the vacuum magnetic permeability, $\vec{M}$ is the magnetization of the standard sample, $\vec{r}$ is the displacement vector between the dipole moment $\vec{m}$ and the volume element dV of the sample, and $\hat{r} = \vec{r}/r$ is the unit displacement vector. The magnetic force gradient is then given by
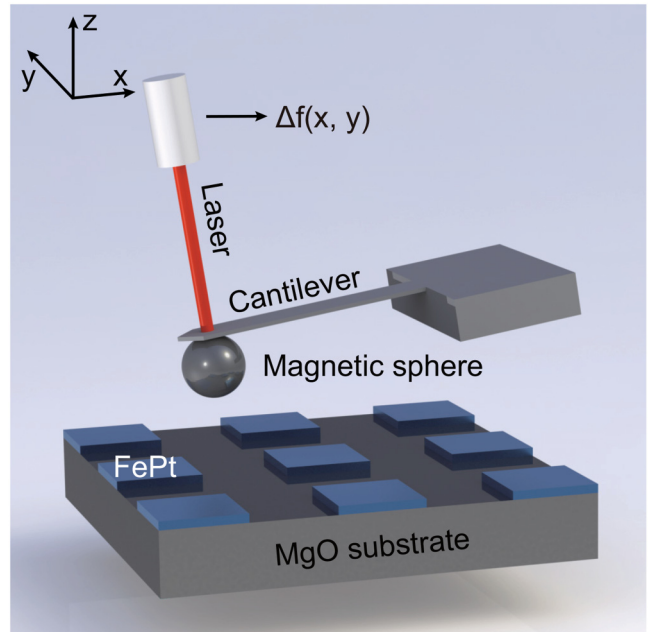

FIG. 1. Schematic diagram of the experiment.

$$\frac{\partial F}{\partial z} = \frac{\partial^2 B_x}{\partial z_m^2}m_x + \frac{\partial^2 B_y}{\partial z_m^2}m_y + \frac{\partial^2 B_z}{\partial z_m^2}m_z,\tag{3}$$

which is a linear combination of the components of the dipole moment. Therefore, the frequency shift can be written as

$$\Delta f = G_x m_x + G_y m_y + G_z m_z + \Delta f_0,\tag{4}$$

where $G_l = -(f_0/2k)(\partial^2 B_l/\partial z_m^2)$, with $l = x, y, z$. Δf_0 being the frequency shift of non-magnetic origins, such as the Casimir force, electrostatic force, and measurement offset. According to Eq. (4), the dipole moment can be obtained by analyzing the Δf image with multiple linear regression.

In order to minimize the contribution of the electrostatic force and Casimir force, the probe-sample distance is set to greater than 200 nm, where the magnitude of the electrostatic force and Casimir force is negligible compared to the magnetic force. To set the distance, we first approach the probe to the surface area without magnetic structures with the Z feedback on. The setpoint of Δf used for the tip-approach defines the initial spacing d_0. The probe is then lifted up for certain height Δd for imaging.

The initial spacing d_0 is determined by the electrostatic force calibration method. When an voltage V is applied between the sphere and the sample, the magnetic sphere is subjected to an electrostatic force given by[35]

$$F_e(d) = 2\pi\varepsilon_0(V - V_0)^2\sum_{n=1}^{\infty}\frac{\coth(\alpha) - n\coth(n\alpha)}{\sinh(n\alpha)},\tag{5}$$

where V_0 is the contact potential difference between the sphere and the sample. $\cosh(\alpha) = 1 + d/R$, where R is the radius of the sphere and $d = d_0 + \Delta d$ is the separation between the surfaces. The gradient of the electrostatic force causes a change in the cantilever resonance frequency, which can be expressed as

$$\Delta f(V, d) = B(d) \cdot (V - V_0)^2 + \Delta f_{ne}(d), \qquad (6)$$

where Δf_{ne} is from other contributions unrelated to electrostatic force and independent of V.

The frequency shift is measured by sweeping the voltage V at different lift height Δd from d_0. The $B(\Delta d)$ at every Δd is obtained by fitting the $\Delta f - V$ curve to Eq. (6). The initial spacing d_0 is then obtained by fitting the $B(\Delta d) - \Delta d$ curve to the theoretical formula derived from Eq. (5).

To quantitatively measure its magnetic moment, the microsphere is first glued on the end of a tip-less cantilever as a probe. The surface tilt of the standard sample is then obtained by imaging the area without magnetic structures using the probe. In this area, we also obtain the initial spacing d_0 using the electrostatic calibration procedure described above. Afterward, the probe is lifted up from the initial spacing for a certain distance and then scans over the magnetic structures with Δf recorded simultaneously. To keep the probe-sample distance constant, the surface tilt is compensated during scanning. A typical image is shown in Fig. 4(b), where nearly half of the image is free of magnetic structures. These areas are used for measuring d_0 and the surface tilt.

B. Standard sample

A suitable standard sample is critical for a reliable calibration of the magnetic moment of magnetic spheres. The standard sample should have well-known magnetization so that the stray field can be accurately calculated. Its magnetization should be less susceptible to stray field generated by the magnetic spheres. To fulfill these requirements, we chose FePt films as the base material for making standard samples. The FePt films with a thickness of 10 nm were deposited on the MgO(001) substrate by magnetron sputtering. The FePt films are in the $L1_0$ phase, which has perpendicular magnetic anisotropy so that we can magnetize the sample normal to the surface.[36,37] Figure 2(a) shows its out-of-plane magnetic hysteresis loop, which shows high squareness and near 100% remanent magnetization. The coercive field is 1265 Oe that is larger than the stray field generated by a sphere at a measurement separation of 446 nm.

The FePt film was patterned to arrays of squares by photolithography and ion beam etching. At the final step, the structures were coated with a 53-nm-thick gold layer to prevent oxidation of FePt films and make the surface isoelectronic. The thickness of the gold film was measured with AFM on a control sample mounted with the standard sample during gold deposition. A gold film structure was fabricated on the control sample using photo-lithography and a lift-off method, which was then used for thickness measurement. The dimension of squares as well as the distance between the squares can be optimized according to the size of the magnetic sphere to improve its spatial resolution. For our application, the length of the square was designed to be $4\,\mu$m, and the distance
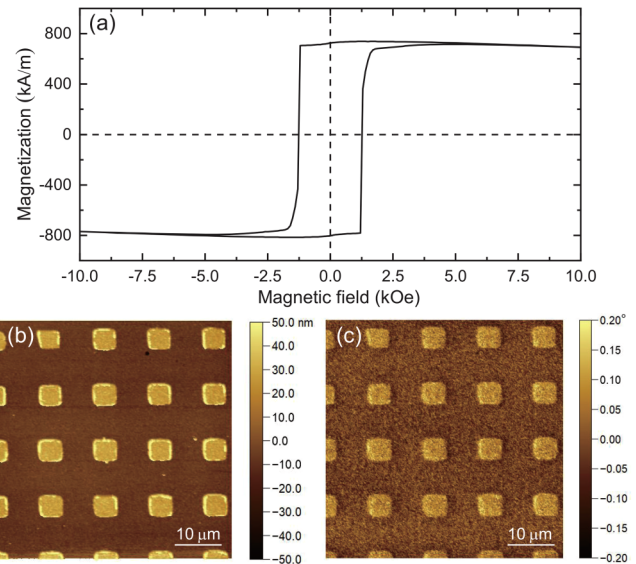

FIG. 2. (a) The out-of-plane magnetic hysteresis loop of the FePt film. (b) The AFM topographic image of the standard sample. (c) The MFM image of the standard sample.

between them is $8\,\mu$m. Figure 2(b) shows a topographic image of the standard sample prior to magnetization, taken with a commercial atomic force microscope (Dimension Edge, Bruker). Afterward, the standard sample was magnetized in a magnetic field of 5 kOe
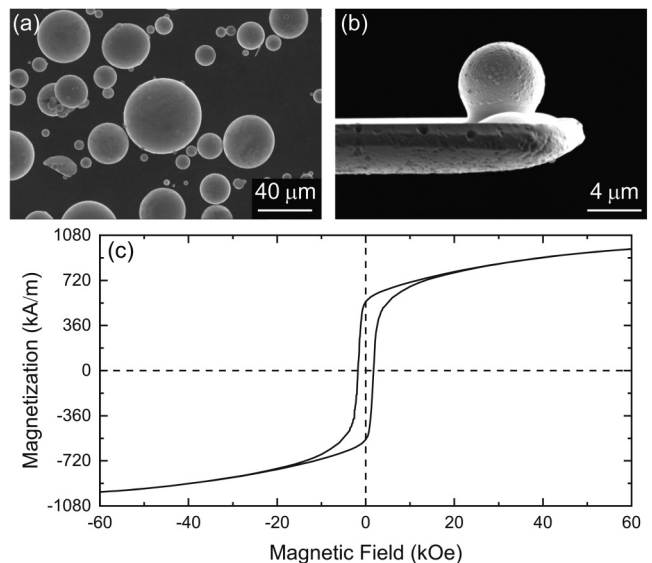

FIG. 3. (a) The SEM image of the NdFeB powder shows magnetic spheres of different sizes. (b) The SEM image of a magnetic probe. (c) The magnetic hysteresis loop of NdFeB powder.
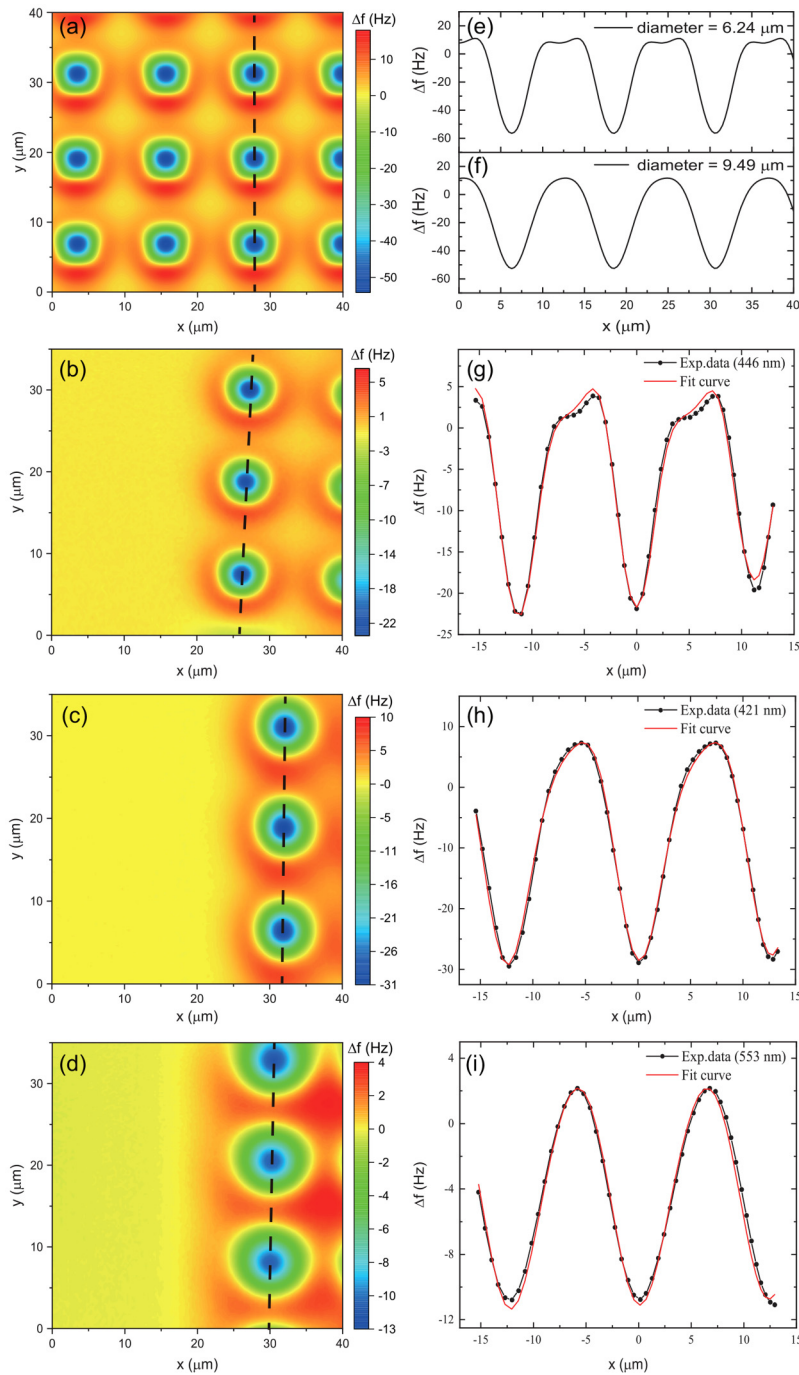
25 December 2023 08:32:57

FIG. 4. (a) The expected Δf image as calculated with $\vec{m} = 6.97 \times 10^{-10}$ A m^2, a separation of 446 nm, and a sphere diameter of 6.24 μm. (b)–(d) MFM Δf images obtained with magnetic spheres of 6.24, 9.49, and 11.96 μm in diameter at separations of 446, 421, and 553 nm, respectively. (e) The line plot of Δf along the dashed line indicated in (a). (f) A calculated line plot of Δf for a sphere with a diameter of 9.49 μm. (g)–(i) The line plots of the experimental data and the fitting curve along the dashed line indicated in (b)–(d).

perpendicular to the surface, and then magnetic force microscopy measurements were taken in the two-pass technique using the same commercial AFM, where the phase shift of the resonance was measured at the second pass [see Fig. 2(c)]. The MFM image is consistent with the single domain nature of the FePt squares with magnetization along the normal direction.

C. Magnetic probes

In this work, we measured the magnetic moment of three NdFeB spheres with different diameters. The magnetic spheres are used as probes to search for exotic interactions beyond the standard of particles.[34] The magnetic properties of individual spheres are important information for the data analysis in those experiments.

The commercially available NdFeB powder (MQP-S-11-9, Magnequench, Inc.) are made of micrometer spheres of different sizes as shown in the scanning electron microscopy (SEM) image [see Fig. 3(a)]. The magnetization curve of NdFeB powder was measured with a SQUID magnetometer [see Fig. 3(c)]. The remanent magnetization is measured to be 548 kA/m. NdFeB sphere of suitable sizes is selected and glued onto single crystalline silicon cantilevers (NSG11/tipless, NT-MDT Spectrum Instruments) under an optical microscope. Figure 3(b) shows a SEM image of a magnetic probe. Its resonance frequency is measured to be 134.64 kHz with a spring constant of 8.13 N/m. The magnetic probe was coated with a gold layer of about 100 nm thick. The sphere was magnetized by applying a magnetic field of 3 T perpendicular to the cantilever.

III. RESULTS AND DISCUSSION

Figure 4(a) shows a Δf image of a theoretical simulation to present the expected characteristics of the measurements. The frequency shift has a dip in the center of the square and show a hump around the edge of the square. Asymmetry can be observed around the center, which is due to the tilt of the sphere's magnetization from the vertical direction [see Fig. 4(e)]. The asymmetry is found to be reduced for spheres with larger diameters due to insufficient spatial resolution [see Fig. 4(f)]. This implies that the method is capable of quantitatively measuring all three components of the dipole moment with the optimal dimensions of FePt patterns.

The experiment was performed on a home-built scanning probe microscope.[38] Figure 4(b) shows an image taken at a separation of 446 nm with a magnetic sphere of 6.24 μm in diameter. The image size is around $40 \times 40 \mu m^2$ (128×128 pixels). The data acquisition time is 30 ms for every pixel. The image presents typical features as expected from the theoretical simulation, such as the periodicity, the dips in the centers, humps around the edges, and the asymmetry around centers.

We obtain the effective dipole moment $\vec{m}$ of the sphere by performing multiple linear regression based on two-dimensional Δf images. The position z of the magnetic dipole can also be optimized by minimizing the residuals in the multiple linear regression analysis using the gradient descent algorithm. In the optimization, the starting position of the dipole is set to the center of the magnetic sphere. Figure 4(g) shows a cut-line plot of the two-dimensional fitting of the Δf image to the theoretical model, and the fitting results are $\vec{m} = (1.89, 0.031, 2.71) \times 10^{-11}$ A m^2 and $z = 407$ nm. The z position of the effective magnetic dipole is 407 nm higer than the center of the sphere. The magnetization is estimated to be 260 kA/m, which is much smaller than the average remanent magnetization measured by the SQUID magnetometer. The measurements of the other two magnetic spheres are presented in Fig. 4, and the fitting results are listed in Table I. We found that the magnetization increases with the diameter of the sphere. As the NdFeB powder is composed of spheres with different diameters around tens of micrometers [Fig. 3(a)], it is reasonable that its average remanent magnetization is 548 kA/m according to our measurements. The diameter dependence of magnetization may be due to oxidation or chemical modification on the surface layer where ferromagnetism is destroyed. Since the ratio of the surface

TABLE I. The magnetic dipole moments and magnetization as measured for different magnetic spheres.

Probe	Diameter (μm)	m_x	m_y	m_z	M (kA/m)
		($\times 10^{-10}$ A m^2)			
1	6.24	0.189	0.003	0.271	260
2	9.49	1.008	0.134	1.476	400
3	11.96	3.887	−0.741	3.888	619

area to volume is large for small microspheres, the average magnetization of the microspheres is expected to decrease as the diameter decreases.

IV. CONCLUSION

In conclusion, we have developed a method to measure the magnetic dipole moment of magnetic particles in micrometer sizes using patterned FePt thin film structures as standard samples. In this method, the FePt features are magnetized to near single-domain magnets in a direction normal to the surface. The standard sample is scanned at constant distance with a cantilever glued with the magnetic particle to be measured, and the frequency shift image is recorded. Multiple linear regression analysis is used to determine the magnetic dipole moment of the particle based on the image. The position of the magnetic dipole moment is further optimized by reducing the residuals in the multiple linear regression analysis. We have performed such measurements on three NdFeB microspheres of different diameters. These spheres will be used as probes to search for new interactions beyond the standard model of particle physics. We found that the magnetization of NdFeB sphere increases with increasing diameter. The method developed in this paper will provide an option to quantitatively characterize magnetic particles using AFM without additional upgrades.

AUTHOR DECLARATIONS

Conflict of Interest

The authors have no conflicts to disclose.

Author Contributions

Rui Luo: Data curation (equal); Formal analysis (equal); Investigation (equal); Writing – original draft (equal); Writing – review & editing (equal). **Qian Wang:** Formal analysis (equal); Methodology (equal). **Yu Lu:** Methodology (supporting); Resources (supporting). **Feng Xu:** Resources (supporting). **Zhe Guo:** Resources (supporting). **Fei Xue:** Resources (supporting). **Long You:** Resources (supporting). **Jinquan Liu:** Validation (supporting); Writing – review & editing (supporting). **Pengshun Luo:**

Conceptualization (lead); Supervision (lead); Writing – review & editing (lead).

DATA AVAILABILITY

REFERENCES

[1]S. B. Smith, L. Finzi, and C. Bustamante, "Direct mechanical measurements of the elasticity of single dna molecules by using magnetic beads," Science 258, 1122 (1992).

[2]O. Kazakova, R. Puttock, C. Barton, H. Corte-León, M. Jaafar, V. Neu, and A. Asenjo, "Frontiers of magnetic force microscopy," J. Appl. Phys. 125, 060901 (2019).

[3]D. Rugar, C. S. Yannoni, and J. A. Sidles, "Mechanical detection of magnetic resonance," Nature 360, 563 (1992).

[4]D. Rugar, R. Budakian, H. J. Mamin, and B. W. Chui, "Single spin detection by magnetic resonance force microscopy," Nature 430, 329 (2004).

[5]E. Nazaretski, K. S. Graham, J. D. Thompson, J. A. Wright, D. V. Pelekhov, P. C. Hammel, and R. Movshovich, "Design of a variable temperature scanning force microscope," Rev. Sci. Instrum. 80, 083704 (2009).

[6]M. Poggio and C. L. Degen, "Force-detected nuclear magnetic resonance: Recent advances and future challenges," Nanotechnology 21, 342001 (2010).

[7]S. H. Chung, A. Hoffmann, S. D. Bader, C. Liu, B. Kay, L. Makowski, and L. Chen, "Biological sensors based on Brownian relaxation of magnetic nanoparticles," Appl. Phys. Lett. 85, 2971 (2004).

[8]Q. A. Pankhurst, N. T. K. Thanh, S. K. Jones, and J. Dobson, "Progress in applications of magnetic nanoparticles in biomedicine," J. Phys. D: Appl. Phys. 42, 224001 (2009).

[9]J. Weizenecker, B. Gleich, J. Rahmer, H. Dahnke, and J. Borgert, "Three-dimensional real-time in vivo magnetic particle imaging," Phys. Med. Biol. 54, L1 (2009).

[10]B. Gleich and J. Weizenecker, "Tomographic imaging using the nonlinear response of magnetic particles," Nature 435, 1214 (2005).

[11]J. Moreland, "Micromechanical instruments for ferromagnetic measurements," J. Phys. D: Appl. Phys. 36, R39 (2003).

[12]M. Weber, R. Koch, and K. H. Rieder, "UHV cantilever beam technique for quantitative measurements of magnetization, magnetostriction, and intrinsic stress of ultrathin magnetic films," Phys. Rev. Lett. 73, 1166 (1994).

[13]C. Rossel, P. Bauer, D. Zech, J. Hofer, M. Willemin, and H. Keller, "Active microlevers as miniature torque magnetometers," J. Appl. Phys. 79, 8166 (1996).

[14]J. G. E. Harris, D. D. Awschalom, F. Matsukura, H. Ohno, K. D. Maranowski, and A. C. Gossard, "Integrated micromechanical cantilever magnetometry of $Ga_{1-x}Mn_xAs$," Appl. Phys. Lett. 75, 1140 (1999).

[15]B. C. Stipe, H. J. Mamin, T. D. Stowe, T. W. Kenny, and D. Rugar, "Magnetic dissipation and fluctuations in individual nanomagnets measured by ultrasensitive cantilever magnetometry," Phys. Rev. Lett. 86, 2874 (2001).

[16]D. P. Weber, D. Rüffer, A. Buchter, F. Xue, E. Russo-Averchi, R. Huber, P. Berberich, J. Arbiol, A. Fontcuberta i Morral, D. Grundler, and M. Poggio, "Cantilever magnetometry of individual Ni nanotubes," Nano Lett. 12, 6139 (2012).

[17]H. C. Overweg, A. M. J. den Haan, H. J. Eerkens, P. F. A. Alkemade, A. L. La Rooij, R. J. C. Spreeuw, L. Bossoni, and T. H. Oosterkamp, "Probing the magnetic moment of FePt micromagnets prepared by focused ion beam milling," Appl. Phys. Lett. 107, 072402 (2015).

[18]F. Xu, S. Guo, Y. Yu, N. Wang, L. Zou, B. Wang, R.-W. Li, and F. Xue, "Method for assembling nanosamples and a cantilever for dynamic cantilever magnetometry," Phys. Rev. Appl. 11, 054007 (2019).

[19]G. A. Gibson and S. Schultz, "A high-sensitivity alternating-gradient magnetometer for use in quantifying magnetic force microscopy," J. Appl. Phys. 69, 5880 (1991).

[20]M. Todorovic and S. Schultz, "Miniature high-sensitivity quartz tuning fork alternating gradient magnetometry," Appl. Phys. Lett. 73, 3595 (1998).

[21]P. Punyabrahma and G. R. Jayanth, "A magnetometer for estimating the magnetic moment of magnetic micro-particles," Rev. Sci. Instrum. 88, 015008 (2017).

[22]T. Göddenhenrich, H. Lemke, M. Mück, U. Hartmann, and C. Heiden, "Probe calibration in magnetic force microscopy," Appl. Phys. Lett. 57, 2612 (1990).

[23]K. L. Babcock, V. B. Elings, J. Shi, D. D. Awschalom, and M. Dugas, "Field-dependence of microscopic probes in magnetic force microscopy," Appl. Phys. Lett. 69, 705 (1996).

[24]L. Kong and S. Y. Chou, "Quantification of magnetic force microscopy using a micronscale current ring," Appl. Phys. Lett. 70, 2043 (1997).

[25]J. Lohau, S. Kirsch, A. Carl, G. Dumpich, and E. F. Wassermann, "Quantitative determination of effective dipole and monopole moments of magnetic force microscopy tips," J. Appl. Phys. 86, 3410 (1999).

[26]R. Yongsunthon, J. McCoy, and E. D. Williams, "Calibrated magnetic force microscopy measurement of current-carrying lines," J. Vac. Sci. Technol. A 19, 1763 (2001).

[27]C. Liu, K. Lin, R. Holmes, G. J. Mankey, H. Fujiwara, H. Jiang, and H. Seok Cho, "Calibration of magnetic force microscopy using micron size straight current wires," J. Appl. Phys. 91, 8849 (2002).

[28]T. Kebe and A. Carl, "Calibration of magnetic force microscopy tips by using nanoscale current-carrying parallel wires," J. Appl. Phys. 95, 775 (2004).

[29]F. Wolny, T. Mühl, U. Weissker, K. Lipert, J. Schumann, A. Leonhardt, and B. Büchner, "Iron filled carbon nanotubes as novel monopole-like sensors for quantitative magnetic force microscopy," Nanotechnology 21, 435501 (2010).

[30]S. Sievers, K.-F. Braun, D. Eberbeck, S. Gustafsson, E. Olsson, H. W. Schumacher, and U. Siegner, "Quantitative measurement of the magnetic moment of individual magnetic nanoparticles by magnetic force microscopy," Small 8, 2675 (2012).

[31]T. Weis, I. Krug, D. Engel, A. Ehresmann, V. Höink, J. Schmalhorst, and G. Reiss, "Characterization of magnetic force microscopy probe tip remagnetization for measurements in external in-plane magnetic fields," J. Appl. Phys. 104, 123503 (2008).

[32]F. Wolny, T. Mühl, U. Weissker, A. Leonhardt, U. Wolff, D. Givord, and B. Büchner, "Magnetic force microscopy measurements in external magnetic fields-comparison between coated probes and an iron filled carbon nanotube probe," J. Appl. Phys. 108, 013908 (2010).

[33]M. V. Rastei, M. Abes, J. P. Bucher, A. Dinia, and V. Pierron-Bohnes, "Field-dependent behavior of a magnetic force microscopy tip probed by means of high coercive nanomagnets," J. Appl. Phys. 99, 084316 (2006).

[34]X. Ren, J. Wang, R. Luo, L. Yin, J. Ding, G. Zeng, and P. Luo, "Search for an exotic parity-odd spin- and velocity-dependent interaction using a magnetic force microscope," Phys. Rev. D 104, 032008 (2021).

[35]B. W. Harris, F. Chen, and U. Mohideen, "Precision measurement of the casimir force using gold surfaces," Phys. Rev. A 62, 052109 (2000).

[36]K. Dong, Z. Guo, Y. Jiao, R. Li, C. Sun, Y. Tao, S. Zhang, J. Hong, and L. You, "Field-free current-induced switching of $L1_0$-FePt using interlayer exchange coupling for neuromorphic computing," Phys. Rev. Appl. 19, 024034 (2023).

[37]R. Li, S. Zhang, S. Luo, Z. Guo, Y. Xu, M. Song, Q. Zou, L. Xi, X. Yang, J. Hong, and L. You, "A spin–orbit torque device for sensing three-dimensional magnetic fields," Nat. Electron. 4, 1 (2021).

[38]J. Wang, S. Guan, K. Chen, W. Wu, Z. Tian, P. Luo, A. Jin, S. Yang, C. Shao, and J. Luo, "Test of non-newtonian gravitational forces at micrometer range with two-dimensional force mapping," Phys. Rev. D 94, 122005 (2016).

25 December 2023 08:32:57